A Modeling Method to Calibrate the Interaction Depth in 3-D Position Sensitive CdZnTe Gamma-Ray Spectrometers

W. Li*, Z. He, G.F. Knoll, D.K. Wehe, Y.F. Du
Department of Nuclear Engineering and Radiological Sciences,
University of Michigan, Ann Arbor, MI 48109, U.S.A.

Abstract

The gamma ray interaction depth in 3-D position sensitive CdZnTe detectors is currently determined by the pulse height ratio of the cathode signal to the anode pixel signal (C/A ratio). In experiments with our 3-D CdZnTe detectors, the photopeak area as a function of the C/A ratio deviates from the expected exponential attenuation with depth. This indicates that the C/A ratio is not proportional to the true interaction depth. This paper proposes a method to calibrate the measured C/A ratio to the interaction depth by modeling the signals from the cathode and anode pixels. Knowing the detector's mobility-lifetime products of the electrons and holes from measurements, the expected pulse heights of the signals from the cathode and anode pixels can be calculated for different interaction depths. The relationship between the C/A ratios and the interaction depths can then be determined and used as the calibration. The calculation for our 3-D CdZnTe detectors shows that an 8% error in depth determination is incurred without the calibration.

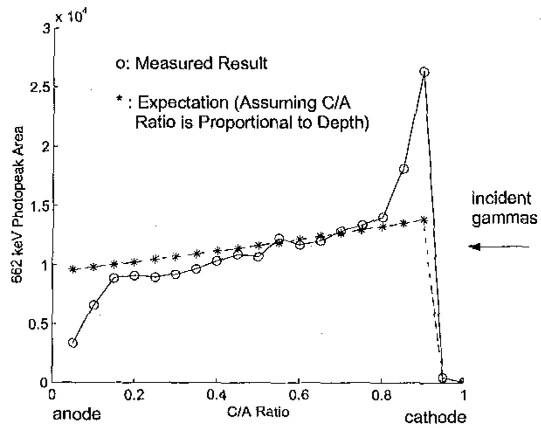

Figure 1: Distribution of 662 keV photopeak area as a function of C/A ratio under -2000 V cathode bias.

I. INTRODUCTION

With 3-D position-sensitive CdZnTe detectors, the interaction location of an incident gamma ray can be uniquely determined in 3-D inside the detector for the single-pixel events[1]. While the lateral location of the interaction is determined by the position of the pixel yielding the signal, the interaction depth is given by the pulse height ratio of the cathode signal to the anode pixel signal (C/A ratio). In experiments with our $1\times1\times1cm^3$ 3-D CdZnTe detectors, the energy spectra of single-pixel events from each pixel are binned into 18~20 depth layers corresponding to equally-spaced intervals of the C/A ratio. Using the measured spectra, the photopeak area as a function of the C/A ratio was calculated. Fig. 1 shows a typical distribution measured using 662 keV photons incident from the cathode side. If the C/A ratio was proportional to the interaction depth, the distribution should resemble the exponential attenuation $e^{-\mu x}$ shown as the dashed line in Fig. 1. The deviation of the measured result from this curve implies that the C/A ratio is not quite proportional to the interaction depth.

In applications such as imaging and material nonuniformity analysis, accurate depth information may be needed. In these cases, the relationship between the C/A ratio and the interaction depth should be well known. While this calibration could be performed with narrow collimation of the γ rays, the difficulty in collimating high energy γ rays and the inconvenience of this method in practice limit its application. To find a more convenient way to do the calibration, a method based on modeling of the signals from the cathode and anode pixel is investigated here. For any given interaction depth, the normalized pulse heights of the signals from the cathode and anode pixel can be calculated from the parameters of the mobilities and mobility-lifetime products of electrons and holes, the weighting potential distribution corresponding to the anode pixel, and other working variables (such as the applied detector bias and shaping time). While the weighting potential that corresponds to the anode pixel can be estimated from the geometry of the electrodes, the mobility-lifetime products of electrons and holes is measured for the material underneath each anode pixel in the experiments. For our 3-D CdZnTe detectors, the mobility-lifetime product of electrons was determined from the measured variation of the photopeak centroid in the energy spectra from the anode pixel[5]. The mobility-lifetime product of holes was determined from the spectrum measured at the cathode for the single-pixel photoelectric events. After all the required parameters are known, the normalized pulse heights of the signals from the cathode and anode pixel can be calculated for any interaction depth. The resulting relationship, between the C/A ratio and the interaction depth can then be is used in the experiments for a corrected interaction depth.

To verify this calculation, the variation of the 662 keV photopeak area as a function of the C/A ratio was calculated for anode pixel spectra from single-pixel events. The result is compared with a measurement and the similarities and differences are discussed.

*E-mail: wenli@engin.umich.edu

0018-9499/00$10.00

II. Modeling the Signals from the Cathode and Anode Pixel

For our 3-D CdZnTe detectors, the signals from the cathode and each anode pixel are read out by a charge sensitive preamplifier, shaping amplifier and pulse height analyzer[3]. To model the output pulse heights from the cathode and anode pixel, we first model the signal current from the electrode due to the charge transportation in the detector, and then model the signal processing through the preamplifier and shaping amplifier.

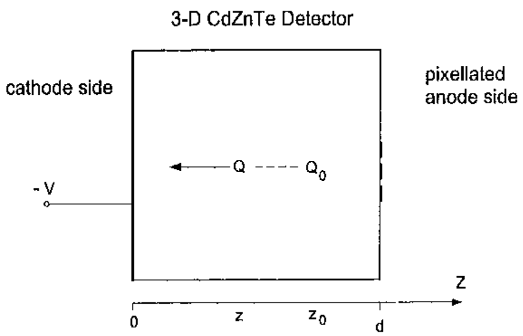

Figure 2: Signal generation in 3-D CZT detector.

A. Signal Current from the Electrode

Consider the situation in Fig. 2. Assume that at time $t = 0$ an electric charge Q_0 is located at depth z_0 in the detector and drifts towards the cathode due to an external electric field. By time $t = T$ the charge is at depth z but has decreased to Q because of charge trapping. On an electrode whose weighting potential distribution is $W(z)$ as a function of the detector depth, at time $t = T$ the signal current induced by the charge's motion is given by:

$$i(z(t)) = Q \cdot dW(z)/dt = Q \cdot \mu \cdot (V/d) \cdot dW(z)/dz \quad (1)$$

Where μ is the mobility of Q, V is the detector bias, and d is the detector thickness. Eqn. 1 assumes a uniform electric field inside the detector. Including the charge trapping associated with the mobility-lifetime product $\mu\tau$, we have (ignoring charge detrapping):

$$i(z(t)) = \frac{Q_0 \cdot \mu \cdot V}{d} \cdot \frac{dW(z)}{dz} \cdot e^{-\frac{|z_0 - z| d}{\mu \tau V}} \quad (2)$$

with

$$z(t) = z_0 - \frac{\mu \cdot V}{d} \cdot t \quad (3)$$

For a γ interaction event in the detector, the signal currents induced by the motion of electrons and holes can be calculated separately using Eqn. 2-3. The overall signal current on an electrode is the sum of the contributions from the electrons and the holes.

The weighting potential for the cathode $W_c(z)$ is linear with the detector depth, and the weighting potential for the anode pixel $W_a(z)$ can be calculated from the geometry of the detector. For our first 3-D CdZnTe detector, the weighting potential distribution for an anode pixel along the path parallel to the detector depth and through the center of this pixel was calculated using COULOMB[2], and the result is shown in Fig. 3 along with the weighting potential for the cathode. The mobilities and mobility-lifetime products of electrons and holes are available from other experiments with the detector, and are discussed later.

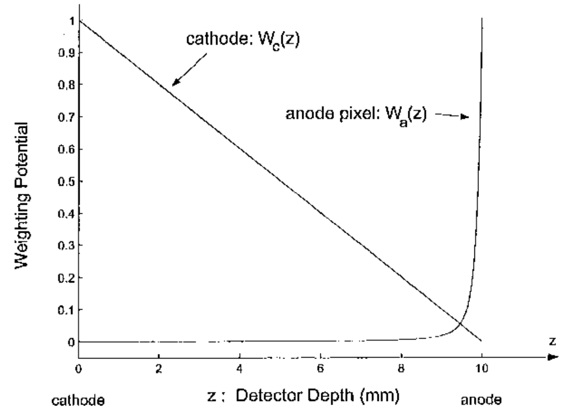

Figure 3: Weighting potentials of the cathode and anode pixel in 3-D CdZnTe detector.

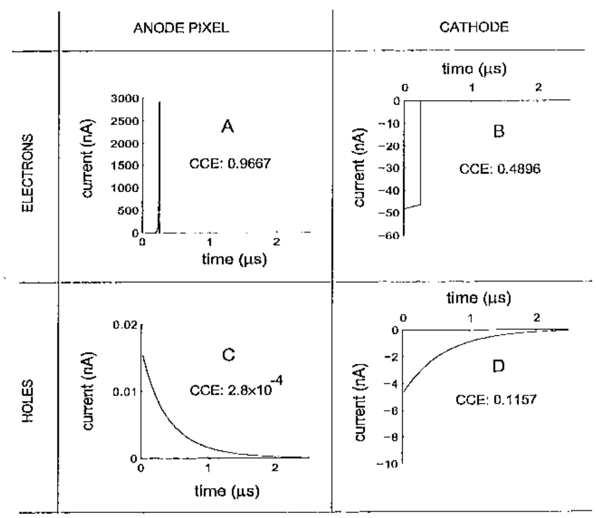

Figure 4: Modeled signal currents and the contributions to charge collection efficiencies for a 662 keV photoelectric event occurring at $z = d/2$. (A) and (C): Contributions to the anode pixel signal from electrons and holes respectively. (B) and (D): Contributions to the cathode signal from electrons and holes respectively.

As an example of the modeling for our 3-D CdZnTe detector (d=10 mm) under the cathode bias of -2000 V, Fig. 4 shows the modeled signal currents from the cathode and collecting anode pixel for a 662 keV photoelectric event occurring at z=5 mm. In the modeling the weighting potentials shown in Fig. 3 are used. Mobilities of (1000, 100) $cm^2/V \cdot s$, and mobility-life time products of $(6 \times 10^{-3}, 6 \times 10^{-5})\ cm^2/V$ are used for electrons and holes respectively. In this example, the contributions from electrons and holes to the charge collection efficiency (CCE) were calculated from integrations of the signal currents, and the results are also shown in Fig. 4.

B. Signal Readout Using Preamplifier and Shaping Amplifier

The charge-sensitive preamplifier and the shaping amplifier can be considered as an integrated signal processing system. The input of this system is the signal current from the detector and the output is the voltage signal from the output of the shaping amplifier. The width of the impulse response function $H(t)$ of this system is determined by the shaping time of the shaping amplifier. If the signal current is constant or the duration of the signal current is much narrower than the width of $H(t)$, the normalized output pulse height of this system is simply proportional to the integration of the signal current (the total charge collected). Otherwise ballistic deficit should be taken into account to get an accurate normalized output pulse height[4]. In the 3-D CdZnTe detector, the duration of the signal current from the cathode depends on the interaction depth, and the average duration time is comparable to the width of $H(t)$. So we could not ignore the signal processing hardware in the modeling. In practice, $H(t)$ is approximated by a Gaussian shape $H(t) = H_0 \cdot e^{-(t-t_0)^2/(2\cdot\tau_s^2)}$ where τ_s is the shaping time of the amplifier. With known $H(t)$ and the signal current $i(t)$ from the detector, the cathode output signal $V(t)$ can be calculated as their convolution:

$$V(t) = i(t) * *H(t) \tag{4}$$

III. Mobility-Lifetime Products of Electrons and Holes

As shown in Eqn. 2, the mobilities and mobility-lifetime products of electrons and holes must be known before $i(t)$ can be calculated. The mobility of electrons μ_e can be estimated from the maximum electron drift time t_{max}:

$$\mu_e = d^2/(V \cdot t_{max}) \tag{5}$$

In the experiment, t_{max} is measured as the maximum rise time from the cathode preamplifier output. For our 3-D CdZnTe detectors, μ_e is measured as 1000 $cm^2/V \cdot s$ using this method. The mobility of holes μ_h is about an order of magnitude smaller than μ_e, so in the modeling μ_h is simply assumed to be 100 $cm^2/V \cdot s$.

The measurement of the electron mobility-lifetime product $(\mu\tau)_e$ can be done using the 662 keV spectra obtained from the anode pixel[5]. From Fig. 3 we can see the 3-D CdZnTe detector exhibits a nearly perfect small pixel effect, which means the pulse height from an anode pixel is only determined by the number of arriving electrons (except for events very near the anode). For the anode spectra which are separated using the C/A ratio, the variation of the photopeak centroid as a function of the C/A ratio indicates the electron trapping along the detector depth and can be used to estimate $(\mu\tau)_e$. The typical $(\mu\tau)_e$ measured by this method from the 3-D CdZnTe detectors is $6\times10^{-3}\ cm^2/V$. Note this value is not exact because our C/A ratio is not yet calibrated to depth z.

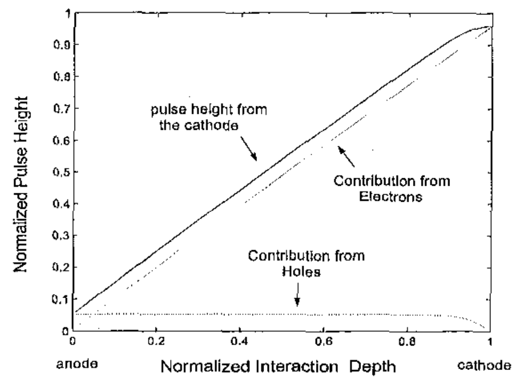

Figure 5: Modeled relationship between cathode pulse height and interaction depth, with -2000 V cathode bias, $(\mu\tau)_e = 6 \times 10^{-3} cm^2/V$, $(\mu\tau)_h = 3 \times 10^{-5} cm^2/V$, $\mu_e = 1000 cm^2/V \cdot s$, $\mu_h = 0.1 \cdot \mu_e$ and the shaping time of 1 μs.

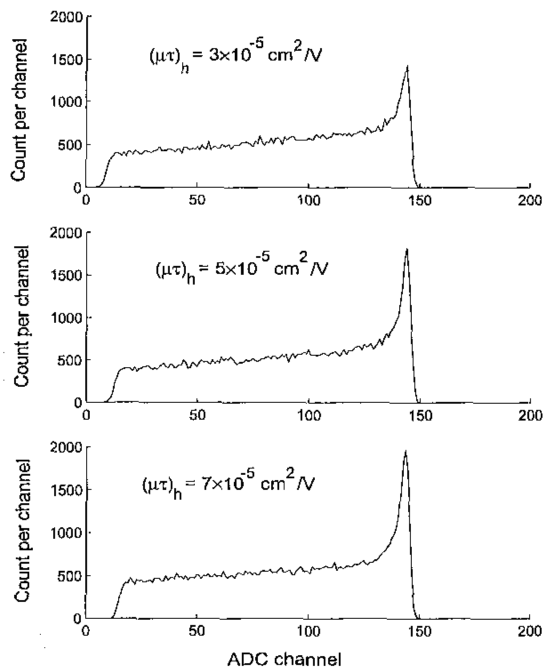

Figure 6: Modeled cathode spectra from 511 keV photoelectric events with -2000 V cathode bias, $(\mu\tau)_e = 6 \times 10^{-3} cm^2/V$, $\mu_e = 1000 cm^2/V \cdot s$, $\mu_h = 0.1 \cdot \mu_e$ and a shaping time of 1 μs.

The measurement of the mobility-lifetime product of holes $(\mu\tau)_h$ is difficult in CdZnTe detectors because $(\mu\tau)_h$ is much smaller than $(\mu\tau)_e$[6]. For the 3-D CdZnTe detectors, $(\mu\tau)_h$ can be estimated by comparing measured and modeled photoelectric spectra from the cathode. With assumed values

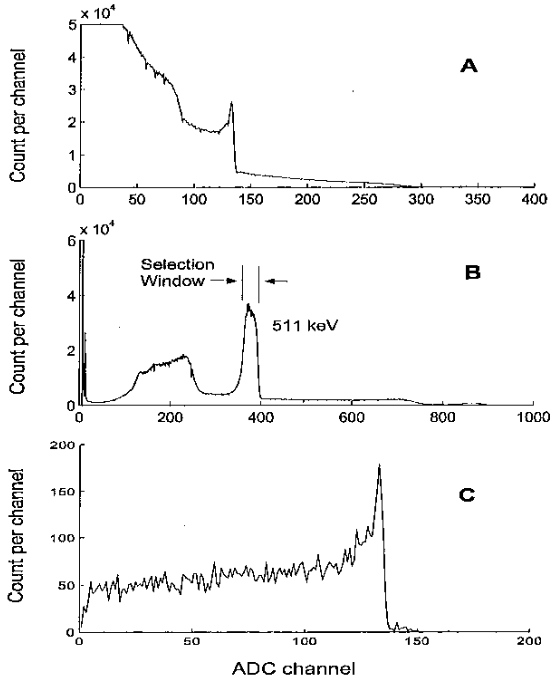

Figure 7: 511 keV Spectra collected from single-pixel events with the 3-D CdZnTe detector under cathode bias of -2000 V. (A). Overall spectrum from the cathode. (B). Overall spectrum from the anode pixel. (C). Cathode spectrum collected from those events within the selection window in (B) and under the anode pixel.

for $(\mu\tau)_e$ and $(\mu\tau)_h$, the cathode pulse heights for the photoelectric events can be calculated for each interaction depth using Eqns. 2, 3 and 4. An example of the modeled relationship between the interaction depth and the normalized pulse height from the cathode is shown in Fig. 5. With the modeled relationship and assumed interaction rate in the detector, the cathode spectrum from the photoelectric events can be calculated. Fig. 6 shows three 511 keV photoelectric spectra from the cathode, modeled with the measured $(\mu\tau)_e$ of 6×10^{-3} cm^2/V and three different values of $(\mu\tau)_h$. In the modeling the γ rays irradiated the detector from the cathode side. The peaks in the spectra in Fig. 6 are from those events near the cathode. Due to the decreasing contribution to the cathode signal from the motion of holes in that region (as shown in Fig. 5), the peaks are sensitive to the variation of $(\mu\tau)_h$. In the experiments with the 3-D CdZnTe detectors, the photoelectric spectrum from the cathode can be measured by admitting only those single-pixel events in the photopeak of the spectrum from the anode pixels. The 511 keV spectra collected in such a measurement is shown in Fig. 7. Spectrum C shows the typical photoelectric spectrum from the cathode for the events underneath an anode pixel. By comparing the peak in spectrum C to those in the three modeled spectra in Fig. 6, $(\mu\tau)_h$ can be estimated as 5×10^{-5} cm^2/V for the material under the anode pixel and near the cathode. It should be noticed that the slope in spectrum C also resembles the modeled spectrum well. The smooth measured slope indicates a smooth relationship between the interaction depth and the normalized pulse height from the cathode (e.g., Fig.5), which suggests there is no significant local variation in the contribution of holes to the cathode signal along the detector depth (and the same for $(\mu\tau)_h$) under this anode pixel. This supports the assumption used in the modeling that the value of $(\mu\tau)_h$ is constant in the material under the anode pixel tested.

IV. Modeled C/A Ratio as a Function of the Interaction Depth

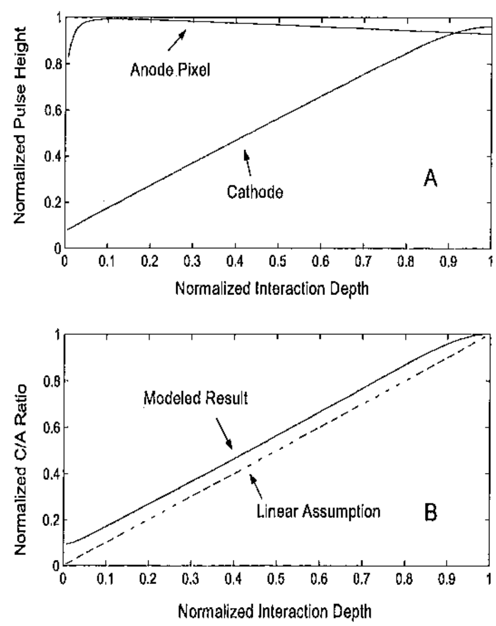

Figure 8: (A). Modeled pulse heights of signals from cathode and anode pixels as a function of interaction depth. (B). Calculated relationship between C/A ratio and interaction depth.

Using the measured $(\mu\tau)_e$ and $(\mu\tau)_h$ of 6×10^{-3} and 5×10^{-5} cm^2/V respectively and assuming a uniform electric field inside the detector, the variation of the normalized pulse heights along the interaction depth can be calculated for signals from both the cathode and anode pixels with a given cathode bias. The results calculated with the typical cathode bias of -2000 V are shown in Fig. 8 (A). The calculated relationship between the C/A ratio and the interaction depth is shown in Fig. 8 (B). Note that assuming the C/A ratio is the normalized depth (dashed curve) will produce an 8% systematic error over most of the interaction depths. In experiments with the same cathode bias, the calculated relation in Fig. 8 (B) can be used to calibrate the measured C/A ratio to the true interaction depth for the single-pixel events in the detector. This calibration relies on the pixel-based measurements of $(\mu\tau)_e$ and $(\mu\tau)_h$ whose results may vary from pixel to pixel. Different calibration curves may be applied to different pixels if there is a significant lateral variation of $(\mu\tau)_e$ and $(\mu\tau)_h$.

With the calibration curve in Fig. 8, the distribution of the γ photopeak area as a function of the C/A ratio can be calculated for the anode pixel spectra from single-pixel events. For 662 keV γ rays irradiating the detector from the cathode side, this distribution was calculated after taking into account the exponential attenuation of the interaction rate along the detector depth and the fluctuations of the signals from the cathode and anode pixel. The final result is shown in Fig. 9. This modeled distribution compares well with the measured one in Fig. 1, except for the minor difference at small C/A ratios. The single-pixel events with small C/A ratios originate from the region near the anode, where the assumption of uniform electric field used in the modeling no longer applies due to the complicated anode pattern and the leakage currents in that region and on the anode surface. A nonuniform electric field would cause a broadened distribution of pulse heights for signals from the same interaction depth and can account for the difference in the modeled and measured results. The overall agreement between the modeled and measured distribution suggests that this calibration method can be applied to the events from most of the interaction depths.

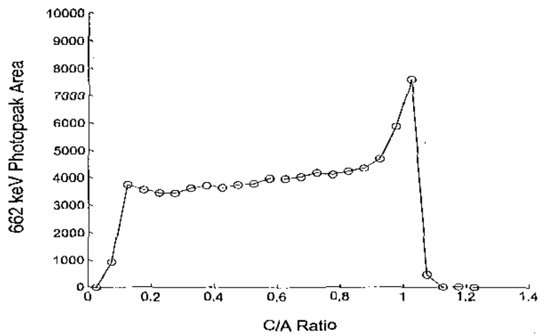

Figure 9: Simulated 662 keV photopeak areas as a function of the C/A ratio. Compare to Fig. 1.

V. Summary and Future Work

For the single-pixel events in the 3-D CdZnTe detectors, a method for calibrating the measured C/A ratio to the true interaction depth is presented in this paper. This calibration is performed by modeling the normalized pulse heights of the signals from the cathode and anode pixels, using the weighting potential and the mobilities and mobility-lifetime products of electrons and holes in the detector. The weighting potential of the anode pixel was calculated from the electrode geometry and the mobilities and mobility-lifetime products of electrons and holes were acquired through other experiments. The normalized pulse heights were modeled for each interaction depth and the resulting relationship between the C/A ratio and the interaction depth can be used as the calibration. The results calculated with cathode bias of -2000 V showed an 8% systematic correction to the interaction depth assuming the measured C/A ratio is the normalized interaction depth. The distribution of photopeak area as a function of the C/A ratio was also modeled and its good agreement with the measured distribution lends credence to the signal generation models used in this calibration method.

The feasibility of this calibration method for the interaction depth will be further investigated with new 3-D position sensitive single carrier detectors. Other calibration methods using the electron drift time and direct γ ray collimation should also be investigated to yield more accurate information about the true interaction depth in the detector.

VI. Acknowledgment

This work was supported under DOE Grant DOE-FG08-98NV13357.

VII. References

[1] Z. He, et al., "3-D Position Sensitive CdZnTe Gamma-Ray Spectrometers", Nucl. Instr. & Meth. in Phys. Res., A 422(1999)173-178.

[2] Integrated Engineering Software, 46-1313, Border Place, Winnipeg, Manitoba, Canada.

[3] W. Li, et al., "A Data Acquisition and Processing System for 3-D Position Sensitive CZT Gamma-Ray Spectrometers", presented at 1998 IEEE Nuclear Science Symposium, to appear in IEEE Trans. Nucl. Sci..

[4] G.F. Knoll, "Radiation Detection and Measurement", John Wiley & Sons, New York, N.Y., 2nd Edition, 1989.

[5] Z. He, et al., "Measurement of Material Uniformity using 3-D Position Sensitive CdZnTe Gamma-Ray Spectrometers", presented at 1998 IEEE Nuclear Science Symposium, to appear in Nucl. Instr. & Meth. in Phys. Res., A.

[6] A. Ruzin, et al., "Methodology for Evaluation of Mobility-Lifetime Product by Spectroscopy Measurements in CdZnTe Spectrometers", J. Appl. Phys. 82(9), 1 November 1997, pp 4166-4171.